AIAA Paper 2004-2707

A Low Diffusion E-CUSP Upwind Scheme for Transonic Flows

Ge-Cheng Zha*
Dept. of Mechanical and Aerospace Engineering
University of Miami
Coral Gables, Florida 33124
E-mail: zha@apollo.eng.miami.edu

Abstract

The original E-CUSP scheme suggested by Zha and Hu is modified to remove the temperature oscillation with low numerical dissipation. The pressure term in the energy equation dissipation is replaced by the total enthalpy. The scheme has low diffusion to accurately resolve wall boundary layers and to capture crisp shock waves. The accuracy of the scheme is compared with other popularly used upwind schemes. For a supersonic flat plate laminar flow, the wall temperature is precisely predicted by using the modified scheme with first order accuracy on a very coarse mesh. The scheme is also tested for the 1D Sod shock tube problem and a transonic nozzle with oblique shock waves and reflections that do not align with the mesh lines. The test cases show that the modified scheme is accurate, robust and efficient.

1 Introduction

Development of an accurate and efficient numerical scheme for compressible flow governing equations is essential due to the increasing engineering demand for aircraft and spacecraft design[1]. An accurate, efficient and robust upwind scheme used as the Riemann solver to resolve shock waves and wall boundary layers is very important.

To achieve the purpose of efficiency and accuracy, efforts have been made to develop upwind schemes only using scalar dissipation instead of matrix dissipation such as that of the Roe's flux difference splitting (FDS) scheme [2]. The examples include AUSM family schemes of Liou [3, 4, 5, 6, 7], the Van Leer-Hänel scheme[8], Edwards's LDFSS schemes[9, 10], Jameson's CUSP schemes and limiters[11, 12, 13], and the E-CUSP schemes developed by Zha, et al.[14, 15, 16, 17], etc.

Pioneered by Liou and Steffen[3, 5, 6], the researchers seeking the scalar dissipation primarily follow the guideline that the velocity and pressure should be separated to consider their characteristics representing the physics of the convection and waves. Liou and his colleagues termed their schemes as advection upstream splitting method(AUSM) schemes, and Jameson gave the name of convective upwind and split pressure (CUSP) schemes[11, 12, 13].

The CUSP schemes can be basically categorized to two types, the H-CUSP and E-CUSP[11, 12, 13]. The H-CUSP schemes have the total enthalpy from the energy equation in their convective vector, while

* Associate Professor, AIAA Member

the E-CUSP schemes use the total energy in the convective vector. The Liou's AUSM family schemes, Van Leer-Hänel scheme[8], and Edwards's LDFSS schemes[9, 10] belong to the H-CUSP group. The schemes developed by Zha, et al.[14, 15, 16, 17] belong to the E-CUSP group.

Even though the H-CUSP schemes such as AUSM family schemes have achieved great success, from the characteristic theory point of view, the schemes are not fully consistent with the disturbance propagation directions, which may affect the stability and robustness of the schemes. By splitting the eigenvalues of the Jacobians to convection (velocity) and waves (speed of sound), one will find that the convection terms only contain the total energy[14], which will lead to the E-CUSP schemes.

Zha and Hu recently suggested an E-CUSP schemes, which has low diffusion and can capture crisp shock wave profiles and exact contact discontinuities[17]. The scheme is consistent with the characteristic directions due to the nature of E-CUSP scheme. The scheme shows the highest stability for two shock tube tests problems compared with several other popularly used upwind schemes for the explicit Euler time marching scheme. The scheme also works well when extended to multi-dimensions[17]. However, with more and more applications, it is found that the E-CUSP scheme of Zha-Hu may generate temperature oscillation near the computation boundary, in particular when the mesh is skewed.

This paper proposes a modification by replacing the pressure term with total enthalpy in the dissipation term of the energy equation. The temperature oscillation is removed and low numerical dissipation is achieved. The modified scheme yields more precise wall temperature than the original scheme. The scheme is proved to be accurate, robust and efficient by the cases tested in this paper. This new scheme is also successfully applied to 3D turbulent flows[18].

For the terminology simplicity and following the terms used in the scheme development, the original E-CUSP scheme[17] is named Zha CUSP scheme and the modified scheme is named as Zha CUSP2 scheme.

2 The Numerical Scheme

2.1 Governing Equations

To describe the new scheme, we will begin with the quasi-1D Euler equations in Cartesian coordinates for inviscid flow:

$$\partial_t \mathbf{U} + \partial_x \mathbf{E} - \mathbf{H} = 0 \tag{1}$$

where $\mathbf{U} = S\mathbf{Q}$, $\mathbf{Q} = \begin{pmatrix} \rho \\ \rho u \\ \rho e \end{pmatrix}$, $\mathbf{E} = S\mathbf{F}$,

$$\mathbf{F} = \begin{pmatrix} \rho u \\ \rho u^2 + p \\ (\rho e + p)u \end{pmatrix}, \quad \mathbf{H} = \frac{dS}{dx} \begin{pmatrix} 0 \\ p \\ 0 \end{pmatrix} \tag{2}$$

In above equations, ρ is the density, u is the velocity, p is the static pressure, e is the total energy per unit mass and S is the cross sectional area of the 1D duct. The following state equation is also employed:

$$p = (\gamma - 1)(\rho e - \frac{1}{2}\rho u^2) \tag{3}$$

where γ is the specific heat ratio with the value of 1.4 for ideal gas.

The finite volume method with the explicit Euler temporal integration is used to discretize the governing equations. It yields the following formulation at cell i:

$$\Delta \mathbf{Q}_i^{n+1} = \Delta t[-C(\mathbf{E}_{i+\frac{1}{2}} - \mathbf{E}_{i-\frac{1}{2}}) + \frac{\mathbf{H}_i}{S_i}]^n \tag{4}$$

where $C = 1/(\Delta x S_i)$, n is the time level index. A numerical scheme is needed to evaluate the interface flux:

$$\mathbf{E}_{i+\frac{1}{2}} = S\mathbf{F}_{i+\frac{1}{2}} \tag{5}$$

2.2 The Original E-CUSP Scheme (Zha CUSP)

In [17], the characteristic analysis is given as the foundation to construct the E-CUSP scheme. Here we will directly go to the details of the scheme.

The Zha CUSP scheme is the following:

For $|u| \leq a$,

$$\mathbf{F}_{\frac{1}{2}} = \frac{1}{2}[(\rho u)_{\frac{1}{2}}(\mathbf{q^c}_L + \mathbf{q^c}_R) - |\rho u|_{\frac{1}{2}}(\mathbf{q^c}_R - \mathbf{q^c}_L)] + \begin{pmatrix} 0 \\ \mathcal{P}^+ p \\ \frac{1}{2}p(u + a_{\frac{1}{2}}) \end{pmatrix}_L + \begin{pmatrix} 0 \\ \mathcal{P}^- p \\ \frac{1}{2}p(u - a_{\frac{1}{2}}) \end{pmatrix}_R \tag{6}$$

Where, the interface mass flux is evaluated as:

$$(\rho u)_{\frac{1}{2}} = (\rho_L u_L^+ + \rho_R u_R^-) \tag{7}$$

$$\mathbf{q^c} = \begin{pmatrix} 1 \\ u \\ e \end{pmatrix} \tag{8}$$

$$u_L^+ = a_{\frac{1}{2}}\{\frac{M_L + |M_L|}{2} + \alpha_L[\frac{1}{4}(M_L + 1)^2 - \frac{M_L + |M_L|}{2}]\} \tag{9}$$

$$u_R^- = a_{\frac{1}{2}}\{\frac{M_R - |M_R|}{2} + \alpha_R[-\frac{1}{4}(M_R - 1)^2 - \frac{M_R - |M_R|}{2}]\} \tag{10}$$

α_L and α_R are evaluated as:

$$\alpha_L = \frac{2(p/\rho)_L}{(p/\rho)_L + (p/\rho)_R}, \quad \alpha_R = \frac{2(p/\rho)_R}{(p/\rho)_L + (p/\rho)_R} \tag{11}$$

The interface speed of sound $a_{\frac{1}{2}}$, Mach number, u_L^+, and u_R^+ are evaluated as:

$$a_{\frac{1}{2}} = \frac{1}{2}(a_L + a_R) \tag{12}$$

$$M_L = \frac{u_L}{a_{\frac{1}{2}}}, \quad M_R = \frac{u_R}{a_{\frac{1}{2}}} \tag{13}$$

The pressure splitting coefficient is:

$$\mathcal{P}^{\pm} = \frac{1}{4}(M \pm 1)^2(2 \mp M) \pm \alpha M(M^2-1)^2, \quad \alpha = \frac{3}{16} \tag{14}$$

For $u > a$, $\mathbf{F}_{\frac{1}{2}} = \mathbf{F}_L$; For $u < -a$, $\mathbf{F}_{\frac{1}{2}} = \mathbf{F}_R$

2.3 The Modified Scheme (Zha CUSP2)

The original Zha CUSP scheme has shown excellent capability to capture shock wave and contact discontinuities with low diffusion. The scheme is consistent with the characteristic direction and have demonstrated high stability compared with several other upwind schemes[17]. The scheme also works well when extended to multiple dimensions.

However, with more and more applications of the scheme, it is found that the Zha CUSP scheme may generate temperature oscillations near the computation boundary, in particular when the mesh is skewed.

To cure the temperature oscillation, the coefficient α is modified for the energy equation by replacing the pressure p with the total enthalpy h_t:

$$\alpha_L = \frac{2(h_t/\rho)_L}{(h_t/\rho)_L + (h_t/\rho)_R}, \quad \alpha_R = \frac{2(h_t/\rho)_R}{(h_t/\rho)_L + (h_t/\rho)_R} \tag{15}$$

The total enthalpy is evaluated as:

$$h_t = e + \frac{p}{\rho} \tag{16}$$

The coefficient α controls the numerical dissipation of the scheme. It should be emphasized that the modification of α in eq.(15) is only applied to the energy equation. For the mass and momentum equation, the α must use the original formulations given in eq.(11).

This modification removes the temperature oscillations. The numerical diffusion remains low at stagnation as analyzed in [17] and is also shown by the wall boundary layer results. Extension of the modified scheme to multi-dimensions is straightforward as described in [17]. Even though this modified scheme will not be able to resolve the exact contact discontinuity as the original Zha CUSP scheme, the Sod shock tube case indicates that the Zha CUSP2 scheme can not only capture crisp shock profile, but can also resolve the contact discontinuity very well.

3 Results and Discussion

According to Godunov[19], when there are discontinuities in the solutions, monotone behavior of a solution can not be assured with higher than first order scheme. Hence, for an upwind scheme to be used as a Riemann solver, it is essential to examine the performance of the scheme using first order accuracy. For the following test cases, all the 1D cases and the 2D flat plate laminar boundary layer use 1st order accuracy in space. The transonic nozzle uses 3rd order accuracy for the inviscid fluxes with MUSCL-type differencing[20] and no limiter is used.

3.1 Shock Tubes

3.1.1 The Sod Problem

Fig. 1 to 3 are the computed Sod shock tube solutions using the Zha CUSP2 and Roe scheme with first order accuracy and explicit Euler scheme[21]. The initial solution is at rest with a diaphragm located in the the middle of the shock tube. The pressure on the left side of the diaphragm is 10 times higher than the pressure on the right side. At time level t=0, the diaphragm breaks. A shock wave propagates to the right side of the tube. A contact surface follows the shock tube traveling toward the right side at a lower speed. An expansion wave propagates to the left side of the tube. Since the computation stops before the waves reach either end of the shock tube, the first order extrapolation boundary conditions are used at both ends of the shock tube.

The CFL numbers used for the shock tube computation is 0.95 for both the Roe scheme and Zha CUSP2 scheme. Fig. 1 is the temperature distribution, which shows that Zha CUSP2 scheme captures the shock profile using 3 grid points while the Roe scheme uses 4 grid points. The contact surface profiles resolved by both schemes are very similar.

The velocity and pressure are constant across the contact surface. Fig. 2 and 3 are the pressure and velocity profiles, which show that the contact discontinuity is very well resolved by the Zha CUSP2 scheme. The velocity profile in Fig. 2 clearly shows again that the shock profile resolved by Zha CUSP2 scheme is crisper than that captured by the Roe scheme.

As pointed out in [17], the maximum CFL number limit for the Roe scheme is 0.95. Oscillations will be generated by the Roe scheme when the CFL number is greater than 0.95. The original Zha CUSP scheme can use maximum CFL number to 1.0. For the Zha CUSP2 scheme, when CFL=1.0 is used, all the variables are monotone except that the velocity has a small over shoot before the shock (not shown).

3.2 Entropy condition

This case is to test if a scheme violates the entropy condition by allowing expansion shocks. The test case is a simple quasi-1D converging-diverging transonic nozzle[15, 16]. The correct solution should be a smooth flow from subsonic to supersonic with no shock. However, for an upwind scheme which does not satisfy the entropy condition, an expansion shock may be produced.

For the subsonic boundary conditions at the entrance, the velocity is extrapolated from the inner domain and the other variables are determined by the total temperature and total pressure. For supersonic exit boundary conditions, all the variables are extrapolated from inside of the nozzle. The analytical solution was used as the initial flow field. Explicit Euler time marching scheme was used to seek the steady state solutions. All the schemes use first order differencing.

Fig. 4 is the comparison of the analytical and computed Mach number distributions with 201 mesh points using the scheme of Zha CUSP2, Roe, Van Leer, Van Leer-Hänel, Liou's AUSM$^+$. The analytical solution is smooth throughout the nozzle and reaches the sonic speed at the throat (the minimum area of the nozzle, located at $X/h = 4.22$). It is seen that both the Roe scheme and Van Leer scheme generate a strong expansion shock at the nozzle throat. Both schemes can converge to machine zero (12 order of magnitude) with CFL=0.95 even with the expansion shock waves. The Van Leer-Hänel scheme can not converge even with CFL=0.01. The result plotted in Fig. 4 is the one before it diverges. It shows an expansion shock with the Mach number jumping from 0.74 to 1.42. The AUSM$^+$ also has difficulties to converge for this case. Using CFL=0.05, it managed to reduce the residual by 4 order of magnitude. The solution of the AUSM$^+$ also shows an expansion shock with the Mach number jumping from 0.86 to 1.17.

Similar to the original Zha CUSP scheme, the Zha CUSP2 scheme does not have an expansion shock

wave at the sonic point, but is not smooth due to the discontinuity of the first derivative of the pressure at the sonic point. This is shown as a small glitch at the sonic point in fig. 4. The glitch does not affect the scheme to converge the solution to machine zero with CFL=0.95.

As reported in [15], when the mesh is refined the amplitude of the expansion shock waves is reduced. When the 2nd order scheme is used, the expansion shock waves disappear.

3.3 Wall Boundary Layer

To examine the numerical dissipation of the new scheme, a laminar supersonic boundary layer on an adiabatic flat plate is calculated using first order accuracy. The incoming Mach number is 2.0. The Reynolds number based on the length of the flat plate is 40000. The Prandtl number of 1.0 is used in order to compare the numerical solutions with the analytical solution. The baseline mesh size is 41×31 in the direction along the plate and normal to the plate respectively. The height of the computational domain is 0.82 times of the flat plate length. There are 13 points within the boundary layer.

Fig.5 is the comparison between the computed velocity profiles and the Blasius solution. The solutions of the Zha CUSP2, Roe scheme, and AUSM$^+$, and the original Zha CUSP scheme all agree precisely with the analytical solution. The Van Leer scheme significantly thickens the boundary layer. The Van Leer-Hänel scheme does not improve the velocity profile.

Fig.6 is the comparison between the computed temperature profiles and the Blasius solution. Again, the scheme of Zha CUSP2, Roe, AUSM$^+$, and the original Zha CUSP accurately predict the temperature profiles and the computed solutions basically go through the analytical solution. Both the Van Leer scheme and the Van Leer- Hänel scheme significantly thicken the thermal boundary layer similarly to the velocity profiles.

Table 1 shows the wall temperature predicted by all the schemes using the baseline mesh and refined meshes. The Zha CUSP2 scheme, the Roe scheme, AUSM$^+$, and the original Zha CUSP scheme predict the wall temperature accurately with the very coarse baselines mesh of 40×30. For the scheme of Zha CUSP2, Roe, and AUSM$^+$, the baseline wall temperature is converged based on the mesh size. For the baseline coarse mesh, the original Zha CUSP scheme predicts the wall temperature with a slightly larger error than that of the Zha CUSP2 scheme. For the baseline coarse mesh, the largest error for the wall temperature prediction is from the Van Leer- Hänel scheme. However, the Van Leer- Hänel scheme predicts the wall temperature precisely when the mesh is refined and the solution is converged to the accurate solution. The Van Leer scheme converges to the wall temperature with the error of 1.8%, which is the largest among the schemes tested. Even though the Van Leer- Hänel scheme predict the wall temperature accurately on the refined mesh, the overall temperature and velocity profiles are as poor as those of the Van Leer scheme even on the refined mesh[17]. When the 2nd order schemes are used, both the velocity and temperature profiles of the Van Leer scheme and Van Leer- Hänel are improved (not shown).

3.4 Transonic Converging-Diverging Nozzle

To examine the performance of the new scheme in two-dimensional flow and the capability to capture the shock waves which do not align with the mesh lines, a transonic converging-diverging nozzle is calculated as inviscid flow. The nozzle was designed and tested at NASA and was named as Nozzle A1[22]. Third order accuracy of MUSCL type differencing is used to evaluate the inviscid flux with no limiter.

Fig.7 is the computed Mach number contour using the original Zha CUSP scheme and the Zha CUSP2 scheme with the mesh size of 175×80. The nozzle is symmetric about the centerline. Hence only upper half of the nozzle is calculated. The upper boundary uses the slip wall boundary conditions and the lower boundary of the center line uses the symmetric boundary conditions. The Mach contours lines computed

Scheme	40×30	80×60	160×80	error
Blasius	1.8000	1.8000	1.8000	0.0
Zha CUSP	1.8061	1.8022	1.8018	0.1%
Zha CUSP2	1.7980	1.7991	1.7988	-0.06%
Roe scheme	1.7990	1.8002	1.7996	-0.02%
Liou $AUSM^+$	1.7993	1.8000	1.8000	0.0
Van Leer	1.8157	1.8328	1.8333	1.8%
Van Leer-Hänel	1.7766	1.7970	1.7996	-0.02%

Table 1: Computed non-dimensional wall temperature using first order schemes with the baseline mesh and refined meshes

by the two schemes look very much the same. However, if we zoom in the temperature contours near the wall, it can be seen that the temperature contours computed by the Zha CUSP scheme has large oscillations as shown in Fig. 8, (a). The oscillations are removed by the Zha CUSP2 scheme as shown in Fig. 8, (b).

As indicated by the wall surface isentropic Mach number distribution shown in fig.9, the flow is subsonic at the inlet with the Mach number about 0.4 and is accelerated to sonic at the throat, and then reaches supersonic with Mach number about 1.35 at the exit. Fig.7 shows that right after the throat, an expansion fan emanates from the wall and accelerates the flow to reach the peak Mach number about 1.5 (fig.9). Due to the sharp throat turning, an oblique shock appears immediately downstream of the expansion fan to turn the flow to axial direction. The two oblique shocks intersect at the centerline, go through each other, hit the wall on the other side, and then reflect from the wall. Such shock pattern is repeated to the exit and the shock strength is weakened with the flow going downstream. Fig. 9 shows that the isentropic Mach number distributions predicted by the new CUSP scheme and the Roe scheme agree fairly well with the experiment. The Zha CUSP2 scheme and the Roe scheme have virtually indistinguishable results.

For this transonic nozzle with the mesh size 175×80 on an Intel Xeon 1.7Ghz processor, the CPU time per time step per node to calculate the inviscid flux is $2.5871 \times 10^{-6} s$ for the new scheme, which is about 25% of the CPU time of $1.0284 \times 10^{-5} s$ used for the Roe scheme. This is a significant CPU time reduction.

This scheme is also successfully applied to 3D turbulent flows and is shown to be accurate, robust and efficient[18].

4 Conclusions

The original E-CUSP scheme suggested by Zha and Hu is modified to remove the temperature oscillation with low numerical dissipation. The pressure term in the energy equation dissipation is replaced by the total enthalpy.

For the 1D Sod shock tube problem using Euler explicit scheme, the modified scheme achieves crisper shock profile than that of the Roe scheme. The contact discontinuity is well resolved. For a quasi-1D transonic nozzle, all the other schemes tested generate expansion shocks at the sonic point. The new scheme does not have the expansion shock even though it has a glitch at the sonic point, which is due to the discontinuity of the first derivative of the pressure splitting at sonic point.

For a Mach=2.0 supersonic adiabatic laminar flat plate boundary layer, the new scheme is able to accurately resolve the boundary layer velocity and temperature profiles using the first order differencing. The solution is as accurate as that of the Roe scheme and the AUSM$^+$ scheme and hence demonstrates the low diffusion of the new scheme.

For a transonic converging-diverging nozzle, oblique shock waves and reflections are crisply captured even though the shock waves do not align with the mesh lines. The predicted wall surface isentropic Mach number distribution agrees well with the experiment. The temperature oscillations generated by the original Zha CUSP scheme is removed. The CPU time for the flux calculation is about 1/4 of the time used by the Roe scheme, which is a significant CPU time saving.

In conclusion, the new scheme is proved to be accurate, robust and efficient for the flow cases tested in this paper.

5 Acknowledgment

This work is partially supported by AFOSR Grant F49620-03-1-0253 monitored by Dr. Fariba Fahroo.

References

[1] P. Roe, "CFD Algorithms." NASA Spring Workshop on Fluids, University of Alabama, Birmingham, Alabama, USA, April 22-24, 2003.

[2] P. Roe, "Approximate Riemann Solvers, Parameter Vectors, and Difference Schemes," *Journal of Computational Physics*, vol. 43, pp. 357–372, 1981.

[3] M.-S. Liou and C. J. Steffen, "A New Flux Splitting Scheme," *Journal of Computational Physics*, vol. 107, pp. 1–23, 1993.

[4] Y. Wada and M.-S. Liou, "An Accurate and Robust Splitting Scheme for Shock and Contact Discontinuities." AIAA Paper 94-0083, 1994.

[5] M.-S. Liou, "Progress Towards an Improved CFD Methods: AUSM$^+$." AIAA Paper 95-1701-CP, June, 1995.

[6] M.-S. Liou, "A Sequel to AUSM: AUSM$^+$," *Journal of Computational Physics*, vol. 129, pp. 364–382, 1996.

[7] M.-S. Liou, "Ten Years in the Making-AUSM-Family." AIAA 2001-2521, 2001.

[8] D. Hänel, R. Schwane, and G. Seider, "On the Accuracy of Upwind Schemes for the Solution of the Navier-Stokes Eqautions." AIAA paper 87-1105 CP, 1987.

[9] J. R. Edwards, "A Low-Diffusion Flux-Splitting Scheme for Navier-Stokes Calculations." AIAA Paper 95-1703-CP, June, 1995.

[10] J. R. Edwards, "A Low-Diffusion Flux-Splitting Scheme for Navier-Stokes Calculations," *Computer & Fluids*, vol. 6, pp. 635–659, 1997.

[11] A. Jameson, "Analysis and Design of Numerical Schemes for Gas Dynamics I: Artificial Diffusion, Upwind Biasing, Limiters and Their Effect on Accuracy and Multigrid Convergence in Transonic and Hypersonic Flow." AIAA Paper 93-3359, July, 1993.

[12] A. Jameson, "Analysis and Design of Numerical Schemes for Gas Dynamics I: Artificial Diffusion, Upwind Biasing, Limiters and Their Effect on Accuracy and Multigrid Convergence in Transonic and Hypersonic Flow," *Journal of Computational Fluid Dynamics*, vol. 4, pp. 171–218, 1995.

[13] A. Jameson, "Analysis and Design of Numerical Schemes for Gas Dynamics II: Artificial Diffusion and Discrete Shock Structure," *Journal of Computational Fluid Dynamics*, vol. 5, pp. 1–38, 1995.

[14] G.-C. Zha and E. Bilgen, "Numerical Solutions of Euler Equations by Using a New Flux Vector Splitting Scheme ," *International Journal for Numerical Methods in Fluids*, vol. 17, pp. 115–144, 1993.

[15] G.-C. Zha, "Numerical Tests of Upwind Scheme Performance for Entropy Condition ," *AIAA Journal*, vol. 37, pp. 1005–1007, 1999.

[16] G.-C. Zha, "Comparative Study of Upwind Scheme Performance for Entropy Condition and Discontinuities." AIAA Paper 99-CP-3348, June 28- July 1, 1999.

[17] G.-C. Zha and Z.-J. Hu, "Calculation of Transonic Internal Flows Using an Efficient High Resolution Upwind Scheme." AIAA Journal, Feb. 2004, (AIAA Paper 2004-1097).

[18] Z.-J. Hu and G.-C. Zha, "Simulation of 3D Flows of Propulsion Systems Using an Efficient Low Diffusion E-CUSP Upwind Scheme." AIAA Paper 2004-3928, 40th AIAA/ASME/SAE/ASEE Joint Propulsion Conference and Exhibit, 11 - 14 July 2004.

[19] S. Godunov, "Finite-Difference Method for Numerical Computation of Discontinuous Solutions of the Equations of Fluid Dynamics," *Mat. Sb.*, vol. 47, pp. 271–306, 1959.

[20] B. Van Leer, "Towards the Ultimate Conservative Difference Scheme, III," *Journal of Computational Physics*, vol. 23, pp. 263–75, 1977.

[21] G. Sod, "A survey of several finite difference methods for systems of nonlinear hyperbolic conversation laws," *Journal of Computational Physics*, vol. 27, pp. 1–31, 1978.

[22] M. L. Mason and L. E. Putnam, "The Effect of Throat Contouring on Two-Dimensional Converging-Diverging Nozzles at Static Conditions ." NASA Technical Paper 1704, 1980.

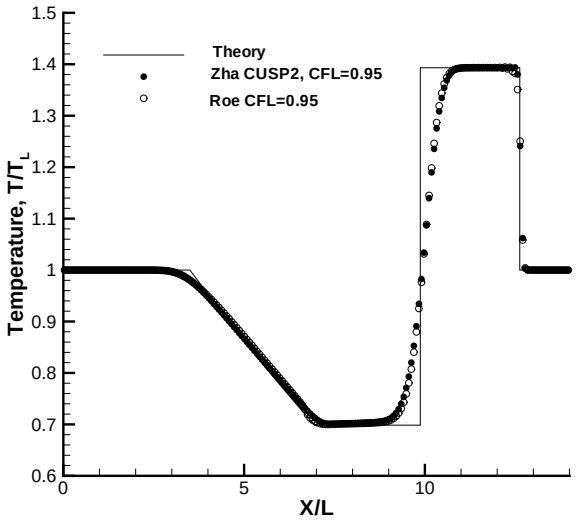

Figure 1: Computed temperature distributions of the Sod 1D shock tube using 1st order schemes

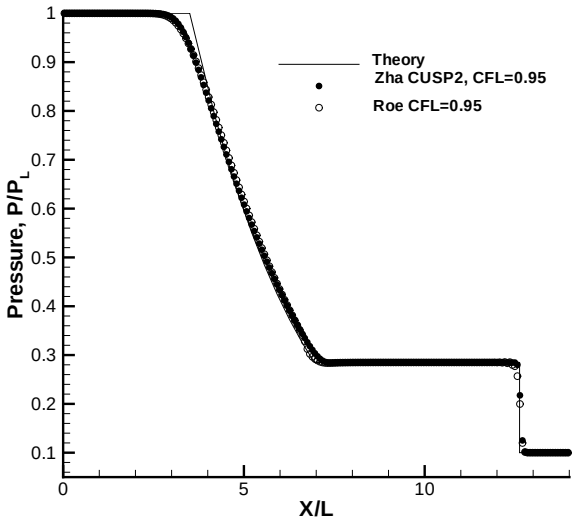

Figure 3: Computed pressure distributions of the Sod 1D shock tube using 1st order schemes

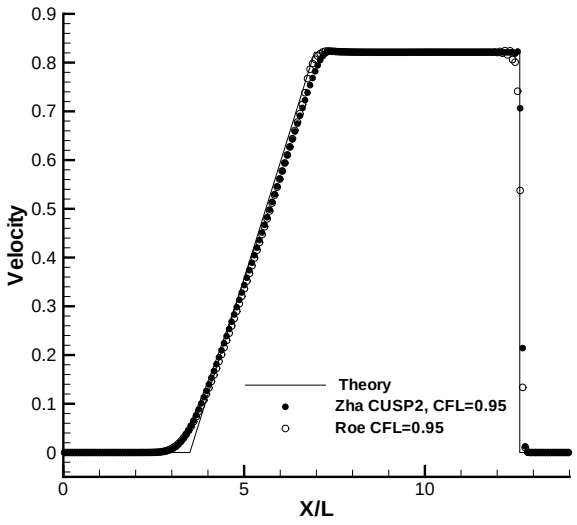

Figure 2: Computed velocity distributions of the Sod 1D shock tube using 1st order schemes

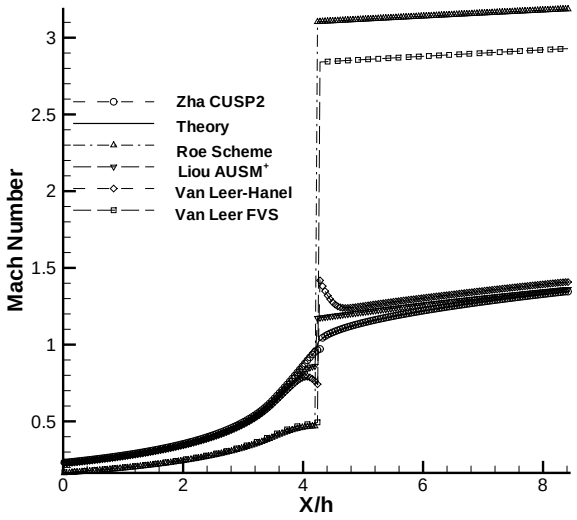

Figure 4: Computed Mach number distributions for the quasi-1D converging-diverging nozzle using 1st order schemes

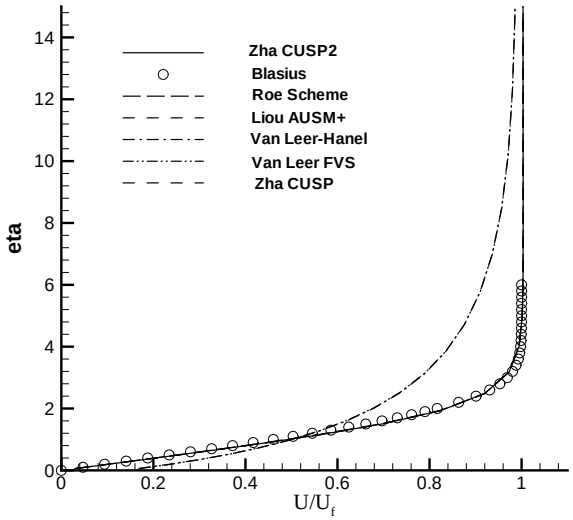

Figure 5: Computed velocity profiles of the laminar boundary layer using 1st order schemes

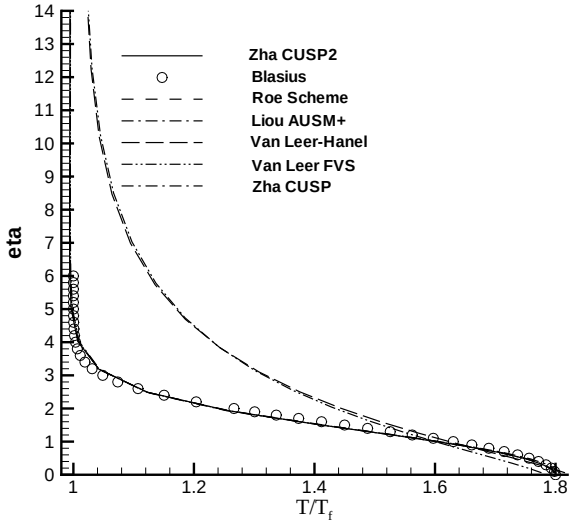

Figure 6: Computed temperature profiles of the laminar boundary layer using 1st order schemes

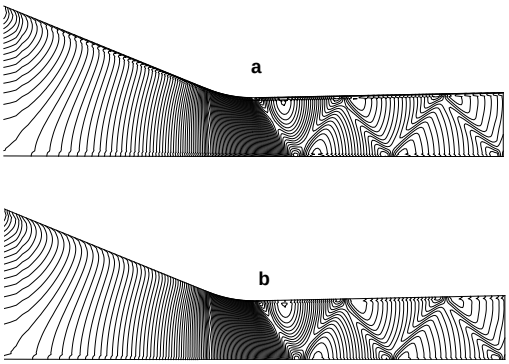

Figure 7: Computed Mach number contours using the Zha CUSP and CUSP2 scheme

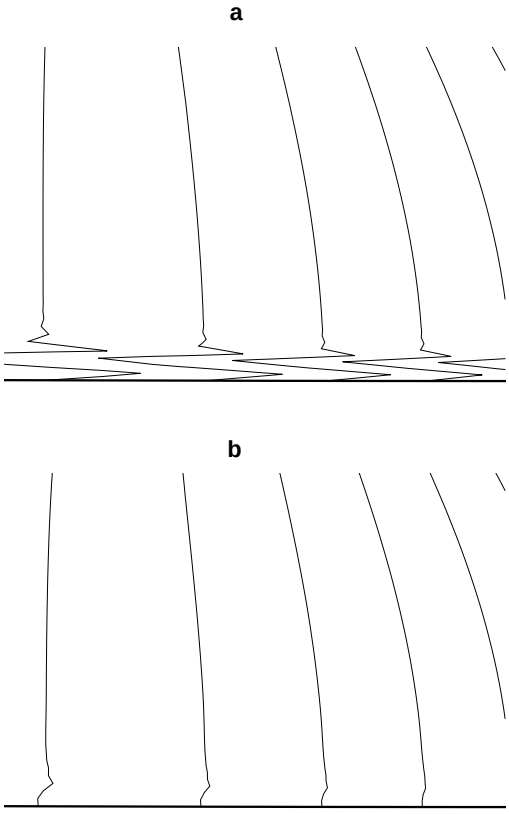

Figure 8: Computed temperature contours using the Zha CUSP and CUSP2 scheme

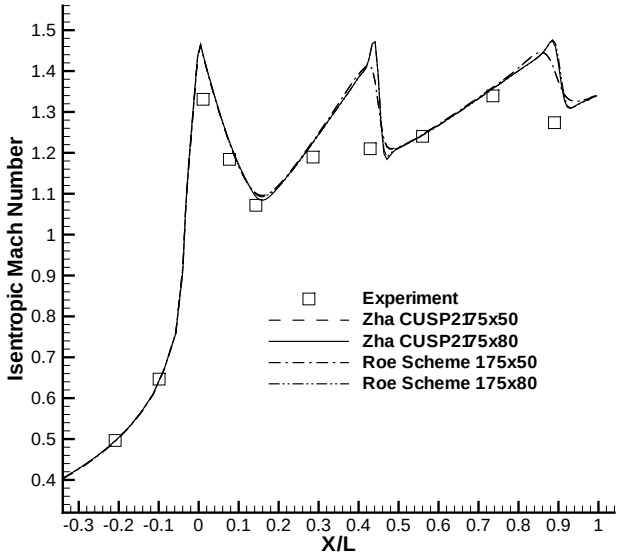

Figure 9: Adiabatic Mach number distribution computed on the wall surface of the nozzle